LA-UR-12-25142

Approved for public release;
distribution is unlimited.

Title:	Experimental Investigation of Bonding Strength and Residual Stresses in LEU Fuel Plates
Author(s):	C. Liu, M.L. Lovato, D.J. Alexander, K.D. Clarke, N.A. Mara, W.M. Mook, M.B. Pime, and D.W. Brown LANL
Intended for:	RERTR 2012 – 34th International Meeting on Reduced Enrichment for Research and Test Reactors, October 14–17, 2012, Warsaw Marriott Hotel, Warsaw, Poland

Form 836 (7/06)

RERTR 2012 — 34th INTERNATIONAL MEETING ON
REDUCED ENRICHMENT FOR RESEARCH AND TEST REACTORS

October 14-17, 2012
Warsaw Marriott Hotel
Warsaw, Poland

Experimental Investigation of Bonding Strength and Residual Stresses in LEU Fuel Plates

C. Liu, M.L. Lovato, D.J. Alexander, K.D. Clarke, N.A. Mara, W.M. Mook,
M.B. Prime, and D.W. Brown
Los Alamos National Laboratory, Los Alamos, NM 87545, USA

ABSTRACT

The interfacial bonding strength and the residual stresses in low enriched uranium fuel plates were investigated experimentally. Controlled-bulge tests were conducted to observe interfacial delamination and determine the associated energy-release rate between hot isostatic pressed (HIP) 6061 Al and Al, and Al and Zr. Mini-cantilever beams were used to investigate the fracture behavior of Al-Zr interfaces, as well as pure Al cantilevers. Deformation was carried out in-situ in the scanning electron microscope, and the load-displacement data were correlated to the observed fracture event. Through-thickness profiles of the longitudinal residual stress were measured with the incremental slitting (crack compliance) method in two clad fuel plates with U-10Mo elements sandwiched between layers of Al 6061. High-energy synchrotron x-ray diffraction was used to profile the residual stresses with 0.1 mm resolution in the U-10Mo foil. The magnitude and location of the largest stresses were determined.

1. Introduction

A significant goal for the Global Threat Reduction Initiative (GTRI) Convert program is converting high performance research reactors from highly enriched uranium (HEU) dispersion fuel plates to low enriched uranium (LEU) monolithic fuel plates. This requires development, qualification, and production of high-density, monolithic LEU-10Mo (wt. pct.) foils [1]. The monolithic fuel foils are to be co-rolled with Zr and clad with 6061Al using hot isostatic pressing (HIP). The resulting fuel plate contains Al-Al, Al-Zr, and Zr-U10Mo bonds whose integrity is critical to performance, including during subsequent processing, shipping, and in-reactor service. The evaluation of the strength and/or toughness of these bonds has proven difficult. Several testing methods have been under development, including bulge testing and mini-cantilever testing, and the current status is discussed in this article.

Due to the mismatch between the coefficients of thermal expansion (CTE), significant residual stress is expected to develop between the aluminum and uranium-molybdenum components of the monolithic fuel element during cooling in the HIP fabrication process. Two techniques were

explored to determine the profile of the residual stress in the fuel plates. Through-thickness profiles of the longitudinal residual stress were measured with the incremental slitting (crack compliance) method in two clad fuel plates with U-10Mo elements sandwiched between layers of Al 6061. The results show mostly compressive stresses in the uranium with balancing tension in the Al, consistent with cooling from the HIP temperature, the thermal expansion mismatch, and the low strength of the Al after the thermal process. High-energy synchrotron x-ray diffraction was used to profile the residual stresses with 0.1 mm resolution in the U-Mo foil. The magnitude and location of the largest stresses were determined. These results will also be briefly discussed.

2. Controlled-bulge test for measuring interfacial toughness of Al/Al and Al/Zr

A technique of using the controlled-bulge test and optical three-dimensional digital image correlation (3D-DIC) was developed to measure the interfacial fracture toughness of an LEU fuel plate. Dannenberg [2] reported the first bulge (blister) test in 1961 for measuring the adhesion of organic coatings to metals or other substrates. In the years that followed, the bulge test has been applied to many systems to study adhesion [3–6]. The analysis of the test is mostly based on plate theory, more specifically the Kirchhoff plate theory [3–5], or membrane theory [6]. The connection of the bulge test with conventional fracture mechanics analysis has also been investigated [7–10].

However, the analysis of the bulge test assumes that the deflected blister experiences elastic deformation and in many cases, the shape of the deforming bulge is assumed to be known and the only unknown is the maximum deflection of the bulge. We applied the 3D-DIC to experimentally determine the profile of the deforming bulge. As a result, our measurement does not depend on any particular plate theory or particular material response, be it elastic or plastic. Thus, we can study a wider spectrum of different material responses.

The controlled-bulge test setup is shown schematically in Fig.1, where two CCD (charge-coupled device) cameras are arranged in front of the testing sample. The entire surface of the bulge has to be “seen” by both cameras in order to measure the shape of the bulge. At each instant of time during the deformation, the 3D profile of the sample surface is quantified. Repeating the process at every instant of time during the test, the evolution of the bulge profile can be obtained, and consequently, evolution of the displacement field on the sample surface can be determined. From the geometric profile of the evolving bulge, the strain field and the curvature field over the bulge surface can be calculated. Such information is necessary for evaluating the mechanical properties of the interface.

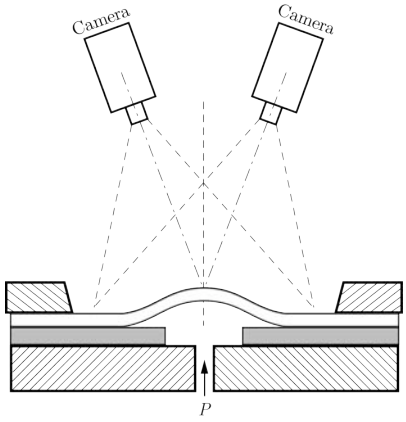

Figure 1: Schematics of controlled-bulge test setup.

Plates of 6061 Al/Al and Al/Zr/Al were made using the same HIP cycle as an LEU fuel plate. Bulge specimens were prepared to observe interface delamination and measure the fracture toughness. Figure 2(a) presents the variation of the applied pressure as a function of the

maximum deflection of the bulge specimen made of Al/Al plate. The evolution of the profile of the deforming bulge is shown in Fig.2(b), where the color represents the out-of-plane motion w of any point normalized by the initial thickness of the Al foil h, at selected moments of time as indicated in Fig.2(a). The bulge profile obtained from 3D-DIC shows apparent enlargement of the bulge boundary, indicating delamination.

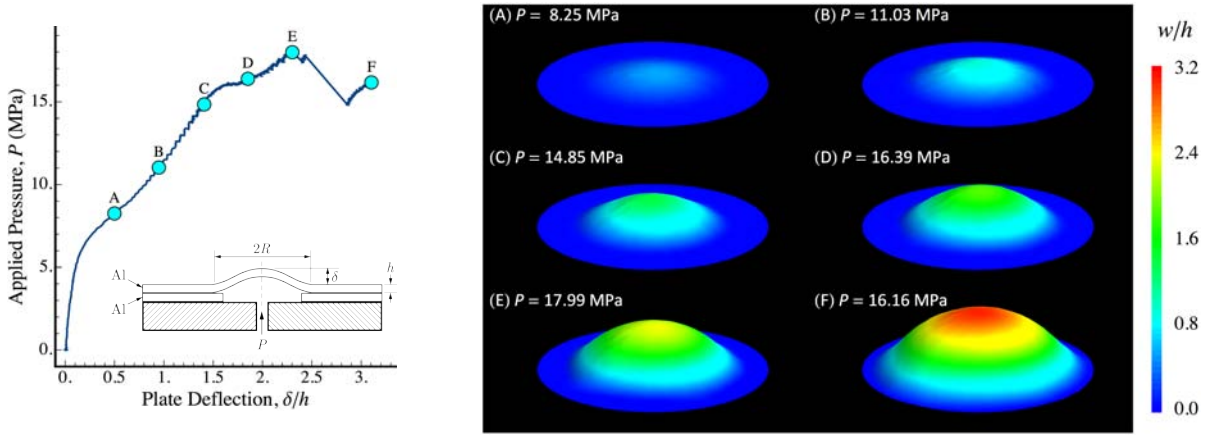

(a) (b)

Figure 2: (a) Variation of applied pressure as a function of the maximum deflection δ of the bulging plate normalized by thickness of the foil h. (b) Profile of the deforming bulge at selected moments of time with associated pressure.

The shape of the bulge, as shown in Fig.2(b), is used to calculate the volume underneath the bulge. The applied pressure is thus established as a function of the bulge volume. Total energy input is the integration of applied pressure over the bulge volume. The strain and curvature fields can also be computed from the displacement field and the profile of the bulge. Note that depending on the ratio of the diameter of the bulge to the thickness of the thin foil, a combination of membrane theory and plate theory is needed in order to describe the strain state at any given point within the bulge. The strain and curvature fields across the bulge surface are sufficient to completely specify the deformation state of the bulge. With the uniaxial tension data of the bulge material, the deformation energy density at any given point of the bulge can be calculated. Integrating the deformation energy density over the thickness of the foil and over the entire surface of the bulge, we obtain the total deformation energy at any given moment during the test. For the Al/Al bulge test, the total energy input E and the deformation energy consumed by the evolving bulge W as a function of deflection of the bulge are shown in Fig.3(a). The flat steps along the curve of the total energy input are due to the fact that during the two unstable pressure drops, shown in Fig.2(a), the applied pressure does no work. We observe that during the early stage of deformation, the deformation energy is equal to the total energy input, which indicates that there is no interfacial delamination occurring. At about δ/h~1.3-1.4, the two energies E and W start to diverge indicating the start of interfacial delamination. The difference between E and W is the energy used for generating new surfaces, i.e., the energy release or delamination energy Π.

One key piece of information for characterizing the delamination of an interface is the quantitative identification of the interfacial crack front or the edge of the deforming bulge. Since 3D-DIC provides complete description of the geometry of the deforming bulge at any given

moment during the process, various parameters that characterize the deformation and geometric features of the bulge can be calculated. To quantitatively identify the boundary or edge of the bulge, we have two different fields to use. One is the mean curvature field κ_{mean} and the other is the minor principal strain field ϵ_2. For a given radial direction, the mean curvature κ_{mean} reaches a maximum at a definite location and these locations form a closed loop. Such a closed loop identifies the edge of the deforming bulge. Similarly, the locations of the minimum minor principal strain ϵ_2 for any given radial direction identify the location of the front of the interfacial crack along the interface. The area within the closed loop can be evaluated and this bulge area is plotted in Fig.3(b) against the deflection of the bulge. Initially, this area equals the area of the recess of the bulge specimen. At about δ/h~1.4, the bulging area A starts to monotonically increase and this matches the moment where the total energy input E and the deformation energy W starts to deviate. Figure 3(c) shows the Al/Al bulge specimen after it was cut open showing that the delamination is indeed along the Al/Al interface.

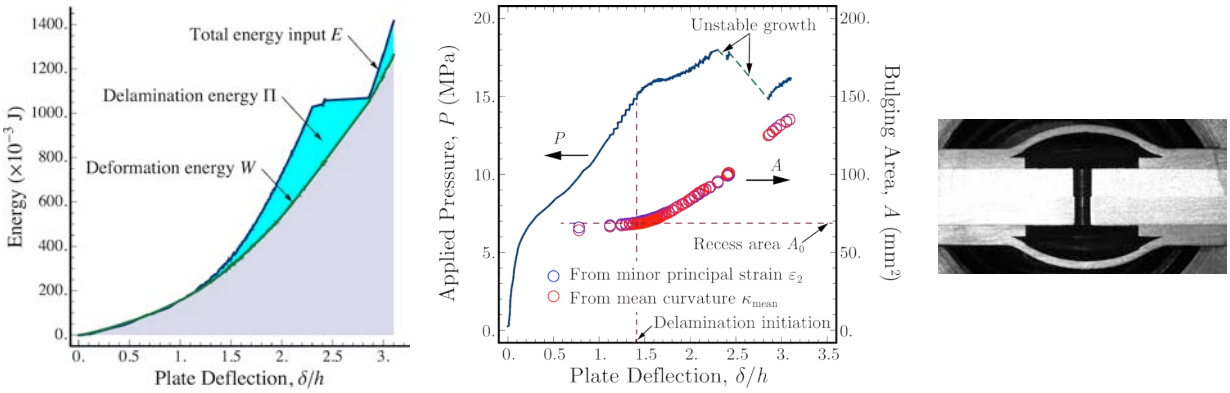

(a) (b) (c)

Figure 3: (a) Energy partition in the controlled-bulge test of the Al/Al interface. (b) Evolution of the area of delamination as a function of the deflection of the deformation bulge. (c) Picture of cut open Al/Al bulge specimen after test showing the delamination is along the Al/Al interface.

Finally, we present the variation of the energy release, or the delamination energy Π, as a function of the bulging area A in Fig.4. The open circles in Fig.4 are from three Al/Al bulge tests and the solid circles are from two Al/Zr bulge tests. The slope of the data shown in Fig.4, $(\partial\Pi/\partial A)/2$, represents the so-called energy-release rate, or the fracture toughness of the interfacial crack. For the Al/Al interface, the average fracture toughness was determined to be 6.39±0.69 mJ/mm^2 and the average fracture toughness for the Al/Zr interface was 4.64±0.06 mJ/mm^2. Figure 4 also shows that the repeatability of the controlled bulge test is quite good.

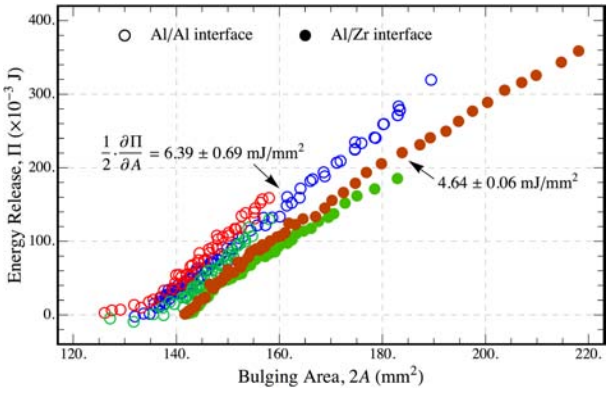

Figure 4: Variation of the energy release, or the delamination energy as function of bulging area of the bulge tests of both Al/Al and Al/Zr interfaces.

We have obtained the interfacial toughness of the Al/Al and Al/Zr interfaces using the controlled bulge test combined with 3D-DIC. We plan to continue to measure the fracture toughness of the Al/U-10Mo interface and also to study the interfaces of the LEU fuel plate prepared with different schemes.

3. SEM *in situ* mini-cantilever beam bending

Recent research into U-10Mo/Zr/Al plate fuel assemblies has illustrated the importance of fundamentally understanding interfacial mechanical behavior. The parameters and phenomena that have been noted include existence of stress gradients at interfaces and their influence on bond strength [11], and strength and fracture behavior of the various interfaces before and after irradiation [12]. Bend testing [13] and pull testing [14] have been used to gain some insight on the mechanical behavior of the composite plate, but as noted in [15], neither method can isolate the mechanical behavior of a specific bond.

The plate geometry specifications [16, 17], include a U-10Mo layer 250 microns thick, a Zr interlayer that is 30 microns thick and Al cladding that is 250 microns thick, with an overall sample thickness of less than 1 mm. As a result conventional macroscopic mechanical tests have had difficulty in providing insight about the mechanical behavior of individual interfaces. In order to give local information about the deformability of the regions in the vicinity of the interface, in this work, micromechanical testing utilizing in-situ deformation in the SEM of small cantilevers was carried out on surrogate HIPed Al/Al and Al/Zr bonds that were processed using HIP parameters typically used for complete U-10Mo/Zr/Al plate fuel assemblies [18].

Experimental:

The mini-cantilever beams were machined with a MiniMill 4 from MiniTech Industries. This equipment has a positioning accuracy of 2.5 μm. This allows the machinist to position an interface at the base of the beam as seen in Fig.7(a). The Al-Al HIP bonded beams were machined to dimensions of 0.75 mm long with a cross-section of 0.25×0.25 mm. The Al-Zr beams were machined to dimensions of 0.3 mm long with a cross-section of 0.1×0.1 mm.

These beams were tested inside of an FEI Quanta scanning electron microscope (SEM) at the Center for Integrated Nanotechnologies (CINT), an international Department of Energy (DOE) user facility at Los Alamos National Laboratory (LANL). The load frame used to test the beams was the in-house built CINT Micromechanical Tester using a 1 N load cell as seen in Fig.5. During testing, the beams were positioned 90° to the SEM electron beam such that the side of the beam and any fracture along the interface in question could be imaged throughout the entire load-unload process. In this way it is possible to monitor interfacial crack

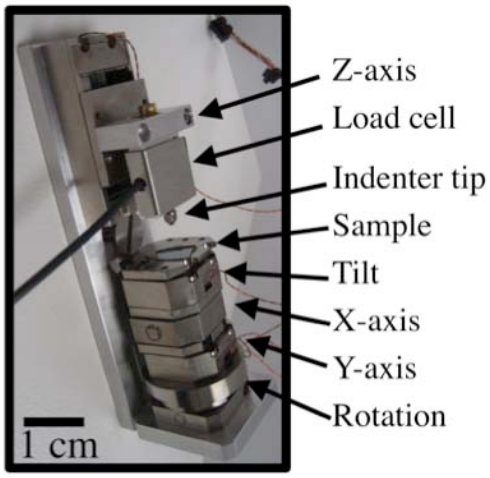

Figure 5: Schematic of custom-built CINT Micromechanical Tester with 1 N load cell used for in-situ straining in the SEM.

length as a function of load in real time. The displacement rate during all of the tests was less than 1 μm/second. The load frame is inherently displacement-controlled, however the displacement rate changes due to compliance of the load cell, i.e., displacement rates during the elastic loading is relatively low while rates during the plastic portion of the bending experiment approach 1 μm/second. Movies of the experiments were created by compiling one image per second from the SEM and synching that to the load-displacement data from the load frame.

Results and Discussion:

The Al-Al HIP interface beams were not pre-notched, and their load-displacement response was very repeatable out of three cantilevers tested. A representative load-displacement curve, along with SEM micrographs of the cantilever before and after testing are seen in Fig.6. It is evident that the beam undergoes significant plastic deformation, with no localized fracture near the interface. From these tests, it is clear that a notch or other stress concentrator is necessary to drive crack propagation at the Al-Al interface. This is consistent with prior work on smaller cantilevers [19, 20] which found that in the absence of stress concentrations such as large inclusions or voids at the interface, the Al-Al bond was as strong as the unbonded material.

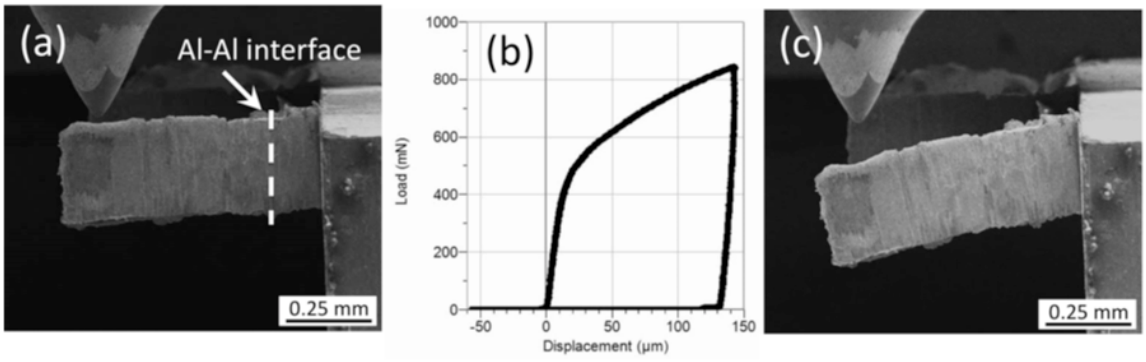

Figure 6: SEM micrographs of the (a) As-milled and (c) deformed Al-Al cantilevers. These samples were not fitted with a pre-notch, and only uniform plastic deformation was observed.

To assure that fracture propagated along the Al-Zr interfaces, these samples were notched with a femtosecond laser. The notches made by the laser varied in depth and proximity to the Al-Zr interface, but were in general within 3 microns of the interface and had a depth of approximately 10 microns. Figure 7 shows the bend test results from an Al-Zr cantilever with a notch located at the Al-Zr interface. Two cantilevers are shown, and in all tests conducted, fracture occurred at the Al-Zr interface. Interestingly, the position of the notch did not seem to affect the path of the crack, as failure always occurred at the Al-Zr interface, even if the notch was located a few microns from the interface itself. This behavior is evident in the cantilever seen in the foreground of Fig.7(c), where the notch was located in the Zr, but fracture still occurred at the Al-Zr interface. From the load-displacement response and the crack length measured via SEM from the in-situ images, fracture energy dissipation rates can be calculated [21].

The fracture energy dissipation rate (D) is:

$$D = \frac{\mathrm{d}U}{\mathrm{d}A} = \frac{1}{2B}\frac{\mathrm{d}U}{\mathrm{d}a};$$

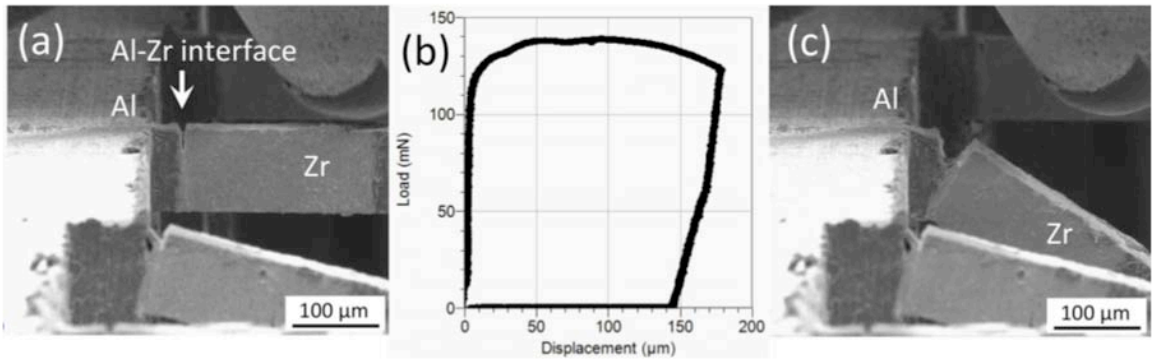

Figure 7: SEM micrographs of the (a) As-milled and (c) deformed Al-Zr cantilevers. These samples were not fitted with a pre-notch, and only uniform plastic deformation was observed. The load displacement curve in (b) corresponds to the labeled cantilever.

where dU is the total energy dissipated, i.e., it is the area under the load-displacement curve. The new surface area of the crack is dA which is the thickness of the beam, B, multiplied by twice the new crack length, $2a$, accounting for the two faces of the crack. It is possible to take images from the SEM movie and calculate D, an example of which can be seen in Table 1.

Table 1: Fracture energy dissipation rate for Al-Zr interface tested in the mini-cantilever beam geometry

a (um)	*da* (um)	*2B*da* (um^2)	*dU* (um*mN)	*D* (mJ/mm^2)
25				
33	8	1600	4416	2.8
39	6	1200	7952	6.6
50	11	2200	9591	4.4

The fracture energy dissipation rate for the Al-Zr interface ranged from 2-7 mJ/mm^2. This is in close agreement with values obtained via bulge testing mentioned earlier in this article. The equation given above assumes an elastic solution to analyze the deformation seen in the test. However, there is clear plastic deformation in the Al phase while the Zr remains elastic, which will certainly affect results. Additionally, throughout the crack growth portions of the load-displacement curve ($a = 25$ to 39 microns), the energy dissipation rate only varies by a factor of 2-3, suggesting that despite varying amounts of plastic deformation in the Al phase as the test progresses, the energy dissipation rate for the system remains the same. This further suggests that the amount of energy dissipated via plastic deformation of Al is very close to that of crack propagation along the Al-Zr interface. In future work, where materials and interfaces embrittled by the effects of radiation are tested, the elastic solution in the above equation should become increasingly applicable.

4. Residual stresses in fuel plates measured by incremental slitting

Through-thickness profiles of the longitudinal residual stress were measured with the incremental slitting (crack compliance) method [22] in two clad fuel plates with U-10Mo elements sandwiched between layers of Al 6061. One plate had 0.61 mm thick U-10Mo off-center in a 4.6 mm total plate thickness, and the other had 0.28 mm thick U-10Mo off-center in a 1.5 mm thick plate. Final data analysis is awaiting characterization of the precise layer

thicknesses at the location of the test. Preliminary results mostly show compressive stresses in the U-10Mo with balancing tension in the Al. The results are generally consistent with cooling from the HIP temperature, the thermal expansion mismatch, and the low strength of the Al after the thermal process. The compressive stresses in the U peak at 100-150 MPa compression at the interface with the Al, and are less than 50 MPa compression in the core of the DU. These number are significantly lower magnitude than the 200 MPa average compression measured by synchrotron in a similar mini fuel plate, but the plates are not identical. The large stress gradients from surface to core in the U-10Mo are indicative of plastic deformation at the Al/U-10Mo interface during cooling from HIP.

5. High-energy x-ray diffraction measurement of residual stresses in monolithic Al/U-10Mo fuel plates

In this study, we profiled the full residual strain tensor of the fuel foil in an aluminum-clad monolithic U-10Mo fuel plate with 0.1 mm spatial resolution using the 1-ID beamline at the Advanced Photon Source at the Argonne National Laboratory. Residual stresses were calculated from the measured strains using the tensoral form of Hooke's law. The largest components of the stress field are in the plane of the foil and compressive, approaching –275 MPa in the longitudinal direction of the fuel assembly at the center of the foil. Predictably, the stress varies rapidly near the transverse edge of the foil. The transverse and longitudinal stresses are not symmetric far from the boundary suggesting that time-dependent and/or plastic deformation of the aluminum as well as the boundary conditions during HIPing also play a role in the development of the residual stresses.

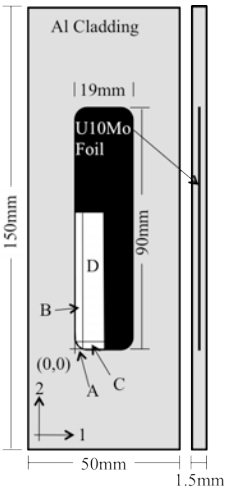

Figure 8: Sample schematic.

A schematic of the sample is shown in Fig.8. The transverse (1) and longitudinal (2) directions of the sample are labeled in the figure and the sample normal direction (3) is out of the page. The dimensions of the U-10Mo foil were 90 mm long, 19 mm wide and 0.28 mm thick and the final dimensions of the fuel assembly was 150×50×1.5 mm.

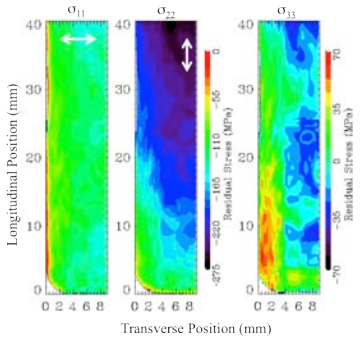

Figure 9: Maps over the studied area of the normal components of the residual stress in the U-10Mo fuel foils in the clad fuel assembly.

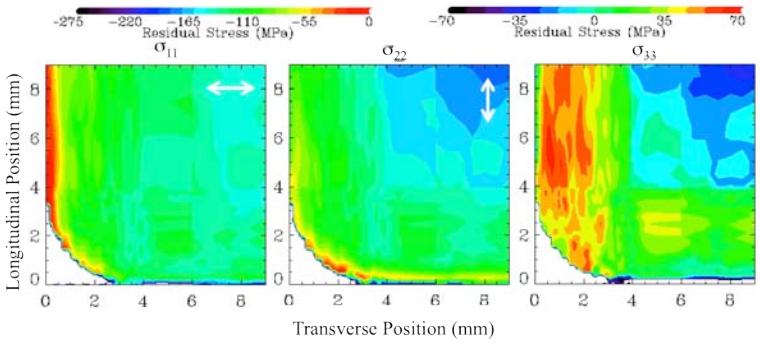

Figure 10: Maps of the normal components of the residual stress in the U-10Mo fuel foils in the clad fuel assembly expanded to highlight the stress gradient near the edge.

Figures 9(a-c) show contour plots of the transverse, longitudinal and normal stresses, respectively, over the portion of the fuel foil profiled with high-energy x-ray diffraction. Note that the scale of the plots of the two in-plane stresses (a-b) is the same and the plot of the normal stress (c) is on a different, smaller, scale. Figures 10(a-c) show an enlarged region of the residual stresses near the corner of the fuel foil. The scales remain as that in Fig.9.

The residual stresses determined with x-ray diffraction do not, in general, agree well with simple elastic estimate or finite element analysis (FEA) [11]. The maximum (absolute) observed residual stress is roughly -275 MPa in the longitudinal direction near the center of the U-10Mo fuel foil. The transverse stress is roughly -120 MPa in the same region. The disparity between the two in-plane stresses near the center of the foil is much larger in the measured data than predicted by the FEA. This suggests that plastic deformation, in particular a gradient in plastic deformation, must be present during cooling. Due to the mismatch in CTE and elastic properties between the fuel and cladding, spatially varying plasticity in the aluminum could result in a stress concentration and complex three dimensional stress state near the edges and corners of the fuel foil, including the presence of significant out-of-plane tensile stresses and high shear stresses.

Acknowledgements

The authors would like to acknowledge the financial support of the US Department of Energy Global Threat Reduction Initiative Reactor Convert program. This work was performed, in part, at the Center for Integrated Nanotechnologies, an Office of Science User Facility operated for the U.S. Department of Energy (DOE) Office of Science. Los Alamos National Laboratory, an affirmative action equal opportunity employer, is operated by Los Alamos National Security, LLC, for the National Nuclear Security Administration of the U.S. Department of Energy under contract DE-AC52-06NA25396. The authors would also like to acknowledge J.K. Baldwin of CINT at LANL for his micromachining expertise in the manufacture of the cantilever beams.

References

[1] D.M. Wachs, C.R. Clark, R.J. Dunavant, *Conceptual Process Description for the Manufacture of Low-Enriched Uranium-Molybdenum Fuel*, Idaho National Laboratory report INL/EXT-08-13840.

[2] H. Dannenberg, “Measurement of adhesion by a blister method,” *Journal of Applied Polymer Science*, **5**, 125–134 (1961).

[3] M.L. Williams, “The continuum interpretation for fracture and adhesion," *Journal of Applied Polymer Science*, **13**, 29–40 (1969).

[4] S.J. Bennett, K.L. DeVries, and M.L. Williams, “Adhesive fracture mechanics,” *International Journal of Fracture*, **10**, 33–43 (1974).

[5] B.M. Malyshev and R.L. Salganik, “The strength of adhesive joints using the theory of cracks,” *International Journal of Fracture Mechanics*, **1**, 114–129 (1965).

[6] J.A. Hinkley, “A blister test for adhesion of polymer films to SiO_2," *Journal of Adhesion*, **16**, 115–126 (1983).

[7] K.M. Liechti and Y.-S. Chai, "Asymmetric shielding in interfacial fracture under inplane shear," *Journal of Applied Mechanics*, **59**, 295–304 (1992).
[8] H.M. Jensen, "The blister test for interface toughness measurement," *Engineering Fracture Mechanics*, **40**, 475–486 (1991).
[9] H.M. Jensen, "Analysis of mode mixity in blister tests," *International Journal of Fracture*, **94**, 79–88 (1998).
[10] Z. Suo and J.W. Hutchinson, "Interface crack between two elastic layers," *International Journal of Fracture*, **43**, 1–18 (1990).
[11] H. Ozaltun and P.G. Medvedev, "Structural behaviour of monolithic fuel plates during hot isostatic pressing and annealing," in *RRFM 2010: 14. International topical meeting on Research Reactor Fuel Management (RRFM),* Marrakech (Morocco), 21–25 March 2010; p. 11.
[12] A.B. Robinson, G.S. Chang, D.D. Keiser, D.M. Wachs, and D.L. Porter, "Irradiation performance of U-Mo alloy based 'monolithic' plate-type fuel," 2009, Idaho National Laboratory.
[13] J.M. Wight, G.A. Moore, and S.C. Taylor, "Testing and acceptance of fuel plates for RERTR fuel development experiments," in *RERTR 2008 International Meeting on Reduced Enrichment for Research and Test Reactors,* Hamilton Crowne Plaza Hotel in Washington D.C., Oct. 5–9, 2008. USA.
[14] D.D. Keiser, J.F. Jue, and D.E. Burkes, "Characterization and testing of monolithic RERTR fuel plates," in *11th International topical meeting. Research Reactor Fuel Management (RRFM) and meeting of the International Group on Reactor Research (IGORR),* Lyon (France), 11-15 March 2007; 2007: France. p. 111.
[15] D.E. Burkes, D.D. Keiser, D.M. Wachs, J.S. Larson, and M.D. Chapple, "Characterization of monolithic fuel foil properties and bond strength," in *11th International topical meeting. Research Reactor Fuel Management (RRFM) and meeting of the International Group on Reactor Research (IGORR),* Lyon (France), 11-15 March 2007; 2007: France. p. 426.
[16] G.A. Moore, B.H. Rabin, J.F. Jue, C.R. Clark, N.E. Woolstenhulme, B.H. Park, et al. "Development Status of U10Mo Monolithic Fuel Foil Fabrication at the Idaho National Laboratory," in *RERTR 2010*. 2010. Lisbon, Portugal.
[17] J. Katz, K. Clarke, B. Mihaila, J. Crapps, B. Aikin, V. Vargas, et al. "Scale-up of the HIP bonding process for aluminum clad LEU reactor fuel," in *RERTR 2011*. 2011. Santiago, Chile.
[18] J.-F. Jue, B.H. Park, C.R. Clark, G.A. Moore, and D.D. Keiser Jr, "Fabrication of monolithic RERTR fuels by hot isostatic pressing," *Nuclear Technology*, **172**, 204–210 (2010).
[19] N.A. Mara, J. Crapps, T. Wynn, K. Clarke, P. Dickerson, D.E. Dombrowski, et al. "Nanomechanical behavior of U-10Mo/Zr/Al fuel assemblies," in *RERTR 2011*. 2011. Santiago, Chile.
[20] N.A. Mara, J. Crapps, T. Wynn, K. Clarke, A. Antoniou, P. Dickerson, et al., Submitted to: *Philosophical Magazine*, (2012).
[21] J.D.G. Sumpter. *Fracture toughness - a measurable materials parameter*. in *Fracture, Plastic Flow And Structural Integrity*. 1 Carlton House Terrace, London Sw1y 5db, England: Iom Communications Ltd.
[22] W. Cheng and I. Finnie, 2007, *Residual Stress Measurement and the Slitting Method*, Springer Science+Business Media, LLC, New York, NY, USA.